

PAPER**CRIMINALISTICS**

*Jimmie C. Oxley,¹ Ph.D.; James L. Smith,¹ Ph.D.; Louis J. Kirschenbaum,¹ Ph.D.;
Suvarna Marimiganti,¹ Ph.D.; Irena Efremenko,² Ph.D.; Raya Zach,³; and Yehuda Zeiri,^{3,4} Ph.D.*

Accumulation of Explosives in Hair—Part 3: Binding Site Study*

ABSTRACT: This study extends previous work on the sorption of explosives to the hair matrix. Specifically, we have studied the interaction of 2,4,6-trinitrotoluene (TNT) and triacetone triperoxide (TATP) as a function of chemical pretreatment with acetonitrile, neutral and alkaline hydrogen peroxide, methanolic KOH and potassium permanganate, and the morphological changes that accompany these treatments. While differences in vapor pressure can account for quantitative differences between TNT and TATP sorption, both are markedly affected by the chemical rinses. Examination of the hair surface shows different degrees of smoothening following rinsing, suggesting that the attachment to hair is largely a surface phenomenon involving the 18-methyleicosanoic acid lipid layer. Density functional theory calculations were employed to explore possible nucleation sites of TATP microcrystals on the hair. We conclude that some of the sites on melanin granular surfaces may support nucleation of TATP microcrystals. Moreover, the calculations support the experimental finding that dark hair adsorbs explosives better than light hair.

KEYWORDS: forensic science, hair, explosives sorption, 2,4,6-trinitrotoluene, triacetone triperoxide, scanning electron microscopy, tapping mode atomic force microscopy

In previous studies of the sorption of explosive vapors by hair (1,2), we made a number of observations that lead to speculation concerning the mechanisms responsible for the sorption of explosives by hair. In the course of our investigations, we noted some general features that have bearing on the potential for forensic analysis of hair from individuals suspected of having contact with explosive materials:

- A general color bias—black and red hair sorbed explosives more readily than brown or blond hair;
- Poor sorption of explosives by bleached hair;
- Poor sorption of explosives by white hair compared to black hair from the same person;
- An individual preference for explosives, that is, if a person's hair sorbed one explosive readily, it sorbed all explosives readily;
- Substantial differences in amount of explosive sorbed by hair compared to cotton balls, wool, polyester, silk, and nylon;
- The observation that high vapor pressure explosives, such as triacetone triperoxide (TATP), appear to be readily rinsed from the surface of hair, but low vapor pressure explosives, such as

2,4,6-trinitrotoluene (TNT), appear to require more vigorous agitation;

- The observation that melanin sorbs both TATP and TNT more readily than some of the best performing black hair;
- Initial sorption of explosive occurs at a rate proportional to the vapor pressure of the explosive;
- Initial sorption of any of the explosives is rapid, but explosive uptake continues at a much slower rate for long periods of time, that is, many months.

Because hair appears to be more than a template on which a subliming explosive can condense, the structure of hair must be considered. Hair structure includes a medulla, an inner cortex, and an outer shell, called the cuticle. Melanin granules, responsible for the hair color, are found almost exclusively in the inner cortex layer. There are two types—eumelanins, the brown-black pigments; and pheomelanins, the yellow-red pigments. The cuticle of hair and, indeed, the outermost layer of skin and nails consist of a fibrous protein known as keratin. However, the outer surface of mammalian hair has a more complex structure than skin or nails. The cuticle is a hard, transparent shingle-like layer made up of 9–10 sheet-like cells, called scales, which are 0.5 μm thick and stacked over each other. Each scale has a laminar structure with an outer and an inner layer, named, respectively, the exo- and endocuticle (3). The epicuticle consists of proteins rich in cysteine, which can cross-link via disulfide bonds to form cystine (4). In hair, this bond occurs about every four turns of the α -helix. Depending on the ethnic origin and the individual, the layers of the cuticle can range from *c.* 7 to 16, resulting in hair diameters from 18 to 180 μm . The surface of the scales is covered by a thin layer (*c.* 3 nm thick) of lipids, the β -layer (4). This layer constitutes a monolayer of saturated fatty acids, the most abundant being 18-methyleicosanoic acid (18-MEA) (5,6). 18-MEA is thought to

¹Department of Chemistry, University of Rhode Island, Kingston, RI 02881.

²Department of Organic Chemistry, Weizmann Institute of Science, 76100 Rehovot, Israel.

³Department of Biomedical Engineering, Ben Gurion University, Beer Sheva 84105, Israel.

⁴Department of Chemistry, NRCN, P.O. Box 9001 Beer Sheva 84190, Israel.

*Funded by Oklahoma City Memorial Institute for Prevention of Terrorism (MIPT), NATO Science for Peace, and the "Center for Security Science and Technology Research Centers" at the Technion, Israel Institute of Technology.

Received 9 Nov. 2010; and in revised form 8 Mar. 2011; accepted 19 Mar. 2011.

be covalently bound, possibly via a thioester linkage, to the cystine-containing proteinaceous outer surfaces of mammalian keratin fibers (7,8). The purpose of this unusual branched-chain fatty acid monolayer is unknown; though, it is speculated that by disrupting the monolayer packing, it imparts beneficial tribological properties.

The interaction of explosives with a multifunctional, biological structure, such as hair, is quite complex. Observations 1, 2, 3, 6, and 7, cited above, suggested that melanin may be involved in sorption of explosives to the hair. However, melanin is found mainly in granules relatively deep in the inner cortex. This study presents experimental data and computational analyses aimed at pinpointing the location of explosive interaction with the hair. In previous work, the computational analysis focused on the reversible and relatively weak sorption, namely physisorption of explosive molecules onto the hair surface governed by van der Waals and Coulomb interactions. Such sorption mechanism does not involve chemical transformations of the adsorbate or the surface. The computations indicated that the thermodynamically stable site for explosive sorption is not the hair protein but the lipid layer, which is modeled as 18-MEA (9). Many of the treatments that affect hair color coincidentally are related to lower the 18-MEA content on the hair surface. Estimations of explosive sorption capacity of the hair surface showed (9) that the experimentally observed TATP sorption onto some types of hair exceeds the monolayer coverage by orders of magnitude. Moreover, it was found experimentally that, in contrast to traditional nitro group-containing explosives, such as, TNT, pentaerythritol tetranitrate, RDX (hexahydro-1,3,5-trinitro-s-triazine), ethylene glycol dinitrate, and nitroglycerin, the peroxide-based explosives TATP and diacetone diperoxide (DADP) can form microcrystalline grains on surfaces of black oriental hair. To explore possible mechanisms that could lead to such behavior of the peroxide-based explosives, density functional theory (DFT) calculations were made to examine the interaction of TATP molecules with different possible active centers on the hair surface and the possible influence of these sites on nucleation of TATP microcrystallines.

Experimental Section

Head hair was obtained by donation or purchased from Demeo Brothers, New York, NY. In the URI laboratory, the hair was rinsed repeatedly with sodium dodecylsulfate (SDS), distilled water, dried, and stored in Ziploc[®] bags (SC Johnson Company, Racine, WI). At BGU, the SDS wash was deleted. TNT was obtained from military sources; TATP was synthesized in the laboratory. All solvents are reagent grade.

Exposure of Hair to Explosives

Hair samples were placed in sealed glass containers such that there was no direct contact with the explosive (1,2). Samples were allowed to stand at room temperature for 48 h. After exposure, the hair was extracted with acetonitrile, and the extracts were analyzed for explosive concentration, as described below. Usually, hair was used only once and then discarded; however, for the sequential exposure tests, after acetonitrile extraction, the hair was dried on a paper towel overnight at room temperature and then re-exposed to the explosive vapors for 48 h.

Special Treatment of Hair

After hair had been cleaned, as described above, it was placed in the desired solvent system and agitated 1–12 h on a shaker (86 shakes/min). Hair was removed from the solvent with forceps

and dried on paper towels overnight at room temperature. The solvent systems used included acetonitrile, methanol, methanol-KOH; KMnO_4 and hydrogen peroxide (H_2O_2), with or without sodium hydroxide. To remove 18-MEA, black hair was immersed in a 0.1 M solution of methanol-KOH (15 mL) and shaken (86 shakes/min) at room temperature for 1 h. Black hair was bleached by soaking overnight in 8% H_2O_2 , both with and without 0.1 M NaOH (an alkaline solution).

Quantification of Explosives Sorption

After exposure to the explosive vapor, the hair samples were divided into three portions (c. 0.05 g each) and weighed into 16-mL amber screw-cap bottles. Acetonitrile (5 mL) was added, and the samples were sonicated for 20 min before being placed on a shaker (speed 86 shakes/min). After shaking overnight, the acetonitrile was removed from the hair using a Pasteur pipette, and 1 mL of solution was put in a 2 mL septum screw-cap vial. All acetonitrile extracts were analyzed on a Hewlett Packard (HP) 5890 gas chromatograph (GC) (Hewlett-Packard Company, Palo Alto, CA) or an Agilent 6890N GC (Agilent Technologies, Santa Clara, CA) using an electron capture detector (ECD) or micro-ECD, respectively. The column used was an Agilent Scientific DB-5MS column (8 m \times 0.53 mm [megabore], film 1.5 μm) or an HP-5 (20 m \times 0.25 mm, capillary column) or a DB-5MS (25 m \times 0.25 mm, capillary column). The injector and detector temperatures were 165°C and 300°C, respectively. Initial and final oven temperatures were 120°C and 220°C, respectively, and hold times were 2 min followed by temperature ramps of 20°/min. An external standard method was used to quantify samples. Standard curves were constructed (using five points between 0.01 and 1.0 ppm) based on peak height and peak area. The squared correlation coefficients for the standard curves were better than 0.99. Both height and area data gave comparable results. Hair from different individuals was first characterized separately and then grouped as to type (see, e.g., Table 1).

Scanning Electron Microscope

A JEOL 5900 scanning electron microscope (SEM) (JEOL, Peabody, MA) was used to study the morphology of untreated and treated black hair. Hair strands were coated with gold before being observed under the microscope and imaged at three or more positions along the fiber. Micrographs were observed at 1000 \times magnification at an accelerated voltage of 15 keV (attempts to use 5000 \times magnification destroyed the samples).

Atomic Force Microscope Measurements

Tapping mode atomic force microscope (TM-AFM) measurements were taken at ambient conditions using a Digital Instrument Dimension 3100 (Digital Instruments Veeco, Santa Barbara, CA) mounted on an active antivibration table. A 100- μm scanner was used. Microfabricated silicon oxide NSC11\50 type tips (ultrasharp) were used. Each measurement was repeated 5–10 times at randomly chosen sites along two different hair samples separated by more than 100 μm . The images were taken in tapping mode with a scan size of up to 20 μm and at a scan rate of 0.5–1.0 Hz. The measurements reported below include height, amplitude, and phase images, allowing us to obtain information about the topology of the scanned areas as well as about the changes in the chemical composition of the scanned area. AFM measurements of hair surface have been reported (10–15). However, to the best of our knowledge, this is the first time that TM-AFM measurements are used to

TABLE 1—Effect of organic solvents on sorption of TATP and TNT by black hair.

Race	Sex	Untreated (48 h)				ACN				MeOH				Untreated (144 h)				ACN				MeOH			
		µg TATP/g Hair		Std Dev	% of Untreated	µg TATP/g Hair Treated		Std Dev	% of Untreated	µg TATP/g Hair Treated		Std Dev	% of Untreated	µg TNT/g Hair Treated		Std Dev	% of Untreated	µg TNT/g Hair Treated		Std Dev	% of Untreated	µg TNT/g Hair Treated		Std Dev	% of Untreated
		Untreated	Treated			Untreated	Treated			Untreated	Treated			Untreated	Treated			Untreated	Treated			Untreated	Treated		
Oriental	M	1630	65	68	2	4	7	2	17	0.6	12	0.6	71	8	0.6	71	8	0.6	71	0.6	71	8	0.6	47	
Oriental	M	1418	192	26	11	14	2	0	24	2.1	18	1.6	74	17	3.0	74	17	3.0	71	1.6	74	17	3.0	71	
Oriental	F								13	2.1	15	0.6	122	14	0.9	122	14	0.9	112	0.6	122	14	0.9	112	
Indian	F	1269	110	50	11	9	3	2	22	3.2	18	3.5	83	19	2.5	83	19	2.5	88	3.5	83	19	2.5	88	
Indian	M	1170	109	180	10	9	3	3	13	2.1	17	0.9	136	23	4.0	136	23	4.0	80	0.9	136	23	4.0	80	
Indian	F	1149	54	54	3	8	7	5	29	0.3	12	1.8	43	26	3.0	43	26	3.0	98	1.8	43	26	3.0	98	
Indian	M	1142	67	19	5	6	1	3	26	3.5	33	5.6	125	22	2.2	125	22	2.2	184	5.6	125	22	2.2	184	
Oriental	F	1055	74	25	8	7	2	3	12	1.5	17	1.5	145	9	1.1	145	9	1.1	57	1.5	145	9	1.1	57	
Caucasian	M	845	107	103	10	13	2	2	15	4.0	16	1.4	107	7	1.0	107	7	1.0	58	1.4	107	7	1.0	58	
Oriental	M	505	51	74	9	10	3	3	12	1.3	8.2	0.4	70	7	1.8	70	7	1.8	34	0.4	70	7	1.8	34	
Oriental	M	699	47	58	4	7	2	4	20	5.7	19	0.3	97	7	1.8	97	7	1.8	34	0.3	97	7	1.8	34	
Indian	F	677	44	98	22	14	2	2	13	0.6	11	0.7	82	15	2.4	82	15	2.4	160	0.6	11	15	2.4	160	
Indian	M	622	18	18	2	15	1	12	9	1.7				11	0.3		11	0.3	72	0.7		11	0.3	72	
Indian	F	165	26	26					15	3.6					0.2			0.2	52					0.2	52
Oriental	M	121	3	3					16	3.5					1.0			1.0	213					2.0	213
Black	M	49	8	11	2	16	0	0	26	1.3					0.2			0.2	72					2.0	72
Black	M	41	34	8	8	83	1	61	10	1.3					1.0			1.0	213					2.4	213
Brown	M	59	37	5	5	62	1	37	10	1.3					1.0			1.0	213					2.4	213
Brown	P	77	22	1	2	29	1	37	10	1.3					1.0			1.0	213					2.4	213
Blond	M	77	22	1	2	29	1	37	10	1.3					1.0			1.0	213					2.4	213

TATP, triacetone triperoxide; TNT, 2,4,6-trinitrotoluene.

investigate the influence of various solvent treatments on the hair surface morphology and composition.

Theoretical Method and Models

DFT calculations were taken using the locally modified version of the GAUSSIAN03 package (16). Detailed description of the computational methods was presented elsewhere (9). Cys and Glu centers on the protein at the hair surface were modeled by single amino acid molecules. The exact structure of melanins has not been fully elucidated (17). However, a new representation of melanin structural model, based upon aggregation of oligomeric units, has been proposed recently, which adequately describes the optical absorption spectrum of eumelanins. Melanins, especially eumelanins, exhibit marked redox properties, and electron delocalization between orthoquinone (OQ) and catecholic moieties of the polymer gives rise to semiquinone (SQ) free radicals, which can be detected by electron spin resonance spectroscopy (18,19). Three monomers—OQ, SQ, and hydroquinone (HQ), shown in Fig. 1—were used to model the melanin centers. Similar models were applied in the DFT study of structure and sorption spectra of eumelanin (10).

Results and Discussion

Effect of Solvent Treatment of Hair on Explosive Sorption

The hair used in these studies was washed and dried prior to use. However, we thought that some of the differences in explosive sorption exhibited by hair of the same color might be due to differences in moisture content. Therefore, some portions of hair were

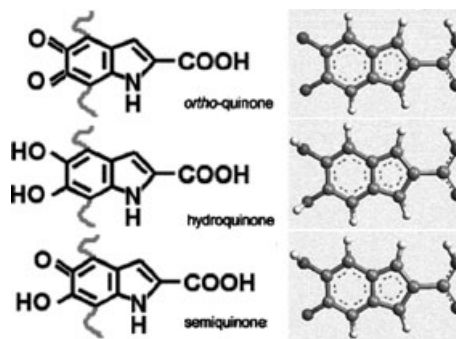


FIG. 1—Structure of indolic melanin (left) and model compounds used to represent key units (right).

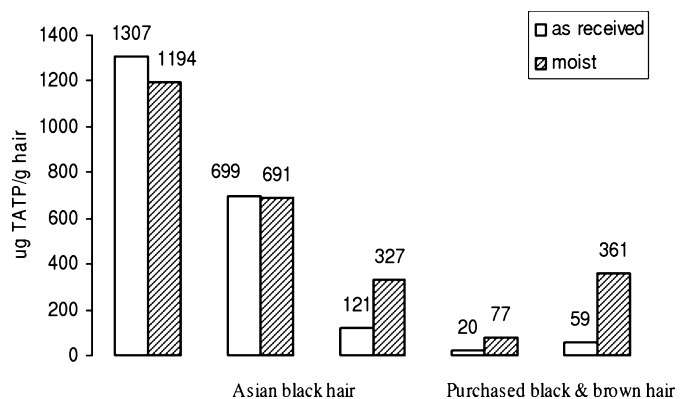


FIG. 2—Effect of moisture on triacetone triperoxide (TATP) sorption.

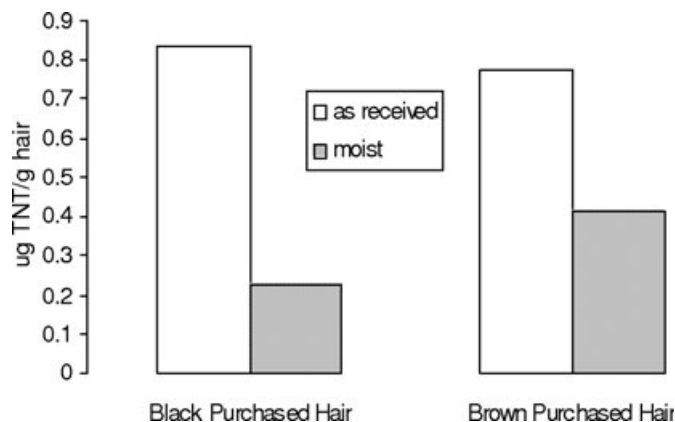


FIG. 3—Effect of moisture on 2,4,6-trinitrotoluene (TNT) sorption.

allowed to stand over water for 48 h. The effects of increased moisture content on TATP and TNT sorption to hair is shown in Figs 2 and 3. Hair that sorbed substantial amounts of TATP (1307 and 699 $\mu\text{g/g}$ hair) did not experience an increase in sorption when moistened (1194 and 691 $\mu\text{g/g}$ hair, respectively), but hair that sorbed TATP poorly, such as the purchased hair, showed increased sorption when moistened. The sorption of purchased hair exposed to TNT was not improved by moisture; in fact its sorption was worsened.

Treatment of Hair with Acetonitrile or Methanol

The usual protocol for hair specimens, after exposure to explosive vapor and extraction with acetonitrile, was to discard the hair. Because we hoped to reuse some of the rarer hair samples, the following experiments were attempted. Instead of discarding the hair after acetonitrile extraction, it was allowed to dry and be re-exposed to the explosive vapor. The reused hair showed an extremely reduced tendency to sorb TATP (Fig. 4). As a result, the effect on TATP and TNT sorption of rinsing hair with acetonitrile or methanol was examined. The treatment with either organic solvent greatly reduced the sorption of TATP by hair that had previously been quite sorptive. Surprisingly, the hair, which initially did not sorb TATP very well (<100 μg TATP/g hair), was not much affected by the organic rinses. Furthermore, the use of organic solvents reduced the degree to which TNT was sorbed only slightly (Table 1).

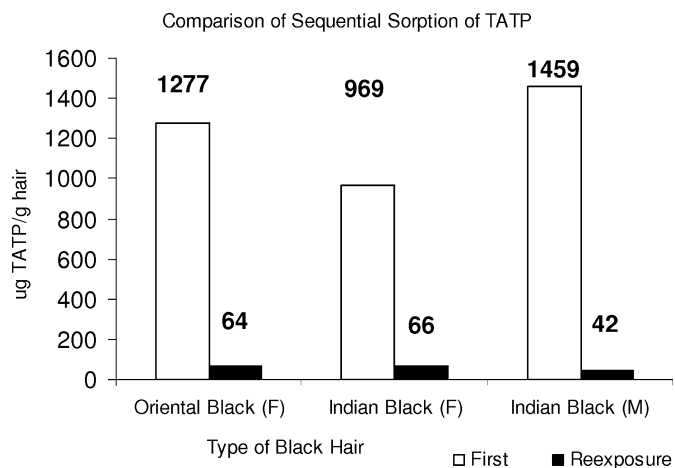


FIG. 4—Black hair: initial sorption of triacetone triperoxide (TATP) over 48 h and results after acetonitrile rinse and re-exposure.

Effect of Hair Color Loss: Graying Hair

We had previously noted that, in general, black hair sorbed all explosives better than brown or blond hair (1,2). Individual variations in hair's sorption ability were observed across all explosives tested, that is, if one sample of hair sorbed an explosive poorly, it sorbed all explosives poorly. Therefore, an effort was made to acquire hair, in this case beard hair, from a person having both white and black hairs. Table 2 clearly shows that the black hair preferentially sorbed the explosives. When black hair was artificially lightened by use of bleach, the bleached hair sorbed substantially less explosive than the unbleached hair (Table 2).

While treatment of hair with organic solvents or water had very different effects on sorption of TATP (decreases it) and TNT (no effect), treatments that affected hair color reduced sorption of both TATP and TNT. Hair color is attributed to melanin, a minor component of hair (c. 2%) found in the cortex. Bleaching agents lighten hair by attacking melanin. However, the oxidation caused by the bleaching agents is not strictly selective for the chromophores in the hair pigment. The bleaching agents can also oxidize the disulfide bonds of the surface proteins. Wolfram et al. (20) demonstrated that although H_2O_2 reacts faster with the hair pigment than the hair protein, it first reacts with the protein because bleaching agent must pass through the cuticle before it encounters the pigment (21,22). Experiments quantifying the rate of reaction of peroxide with pigmented versus nonpigmented hair showed that initially (c. 10 min) the rate of reaction was similar because the initial reaction was with the proteins at the surface of the hair, where no pigment was found. At longer times, pigmented hair degraded peroxide faster. This is presumably due to the requirement that the peroxide needs time to diffuse to the interior of the hair to interact with the hair pigment (20,22,23).

There are a number of potential bleaching agents. In terms of the decolorizing power of the oxidizing agent on melanin, Wolfram et al. (20) ordered the oxidizing agents as permanganate the greatest, H_2O_2 the weakest, and hypochlorite and peracid as intermediate. However, he noted that penetration of the melanin-containing granules was an important consideration and alkaline H_2O_2 was effective in dissolving the granules. There are also a large number of potentially oxidizable sites on the hair protein in the cuticle and cortex. Bleaching with alkaline (NaOH) H_2O_2 or with alkaline peroxide/persulfate has been shown to alter amino acid composition by lowering the cystine and raising the cysteic acid content via oxidation of the disulfide linkages (20,23–25). While it is well known that bleaching oxidizes the cystine residues, there is some controversy whether bleaching also removes 18-MEA. Attempts to remove 18-MEA by completely soaking hair in a methanolic solution of KOH also partially oxidize the cystine groups to cysteic acid (26).

The above discussion suggests that while bleaching may alter explosive sorption by degrading the melanin, it is also likely to

TABLE 2—Sorption by black versus white or whitened hair.

Exposed to Type Hair	TATP 48 h		TNT 940 h	
	TATP ($\mu\text{g/g}$ hair)	Std Dev	TNT ($\mu\text{g/g}$ hair)	Std Dev
Unbleached black	1258	70	214	20
H_2O_2 bleached black	394	66	50	8
NaOH, H_2O_2 bleached black	625	31	73	12
Black hair	645		312	18
White hair	467	26	158	21

TATP, triacetone triperoxide; TNT, 2,4,6-trinitrotoluene.

affect explosive sorption by altering the hair surface. The reason white hair sorbs explosive poorly compared to black is likewise ambiguous. The poor sorption ability of white hair could reflect the lack of melanin, but it has also been reported that gray hair has reduced levels of 18-MEA. Furthermore, the slight ethnic bias in explosive sorption might also be attributed to racial differences in 18-MEA content, African hair having the least. Given these considerations, different hair bleaching methods were used. All methods reduced the ability of hair to sorb both TNT and TATP (Table 3).

Results in Table 3 indicate that TATP sorption was adversely affected by all hair treatments. With the exception of acetonitrile, sorption of TNT was also reduced by the treatment methods. It appears that rinsing of the hair with organic solvent may not have affected TNT sorption at all, but bleaching did reduce its sorption. To accentuate the TNT results, Fig. 5 compares the sorption of untreated to treated hair where TNT vapors are enhanced by holding the exposure chamber at 70°C. These results clearly show that the sorption of TNT is much greater on water-treated hair as compared to methanol-KOH treated hair. These results also suggest the reason purchased hair exhibited poor sorption of both TATP and TNT (Table 1, last four rows), because commercial hair is processed to add gloss and to remove and resist bacterial and insect contamination (e.g., with naphthalene).

Visualization of Hair Surface

Scanning Electron Microscopy

In an attempt to understand how various treatments affected the sorption of explosive by hair, SEM images (1000×) were taken of untreated Asian black hair and the hair treated with various solvents (Figs 6–9). Unfortunately, little difference could be seen between the surfaces of the untreated and the treated black hair. Therefore, TM-AFM was taken.

TM-AFM Measurements

Hair soaked in four different solvent systems, including water, was examined by TM-AFM. Large-area scans of dimensions 20 × 20 μm and 10 × 10 μm were performed. In most cases, these large-area scans covered an area containing more than a single scale. A set of typical results are shown in Fig. 10. Inspection of these images clearly shows that the hair sample rinsed only in distilled water has the roughest surface (top left scan), while the sample treated by methanol-KOH solution is extremely smooth. The samples treated with the other two solvents are rougher than the one rinsed in methanol-KOH, but they are smoother than the one treated by water only. The images in the middle column show the root mean square changes in the cantilever amplitude during the scan. These images tend to enhance edges of the surface examined. This can be clearly observed by the enlarged roughness on the scale surfaces as well as in the transition from one scale to another. The phase images monitor the changes in phase offset of the input drive signal with respect to the phase offset of the oscillating cantilever. The phase offset between the two signals is defined as zero for the cantilever oscillating freely in air. As the tip engages the sample surface, the phase offset of the oscillating cantilever changes by some angle with respect to the phase offset of the input drive signal. When regions with different elasticities are encountered on the sample surface, the phase angle between the two signals is changed. These changes are attributed to different amounts of dumping experienced by the probe tip as it rasters across the sample surface. Again, the largest variation in the phase images is

TABLE 3—Black hair (Asian female): effect of different treatments on explosive sorption.

Type Hair	Explosive	Untreated		CH ₃ CN Only		MeOH Only		0.1 M KOH/MeOH		H ₂ O ₂		H ₂ O ₂ /NaOH		KMnO ₄	
		μg Explosive/g Hair	Std Dev	μg Explosive/g Hair	Std Dev	μg Explosive/g Hair	Std Dev	μg Explosive/g Hair	Std Dev	μg Explosive/g Hair	Std Dev	μg Explosive/g Hair	Std Dev	μg Explosive/g Hair	Std Dev
IF(KB)	TATP	684	28	246	41	—	nd	—	—	—	—	—	—	—	—
OF(HY)	TATP	1258	70	—	—	—	—	—	—	394	66	—	—	—	—
IF(KB)	TNT	20	5.7	19	0.3	7	1.8	4	0.2	—	—	625	31	—	—
IF(SN)	TNT	31	1.2	—	—	—	—	6	0.7	—	—	—	—	—	—
IF(KS)	TNT	36	6.7	40	4.2	—	—	nd	nd	—	—	20	3.5	16	2.4
OF(HY)	TNT*	214	20	—	—	—	—	—	—	50	12.0	73	7.9	—	—

TATP, triacetone triperoxide; TNT, 2,4,6-trinitrotoluene; nd, none detected. TATP exposure was 48 h; TNT was 144 h. TNT* was exposed 940 h. Me/KOH is KOH in 0.1 M methanol; H₂O₂ is 3% peroxide except where * is 8% peroxide; KMnO₄ is a 0.03 M aqueous solution.

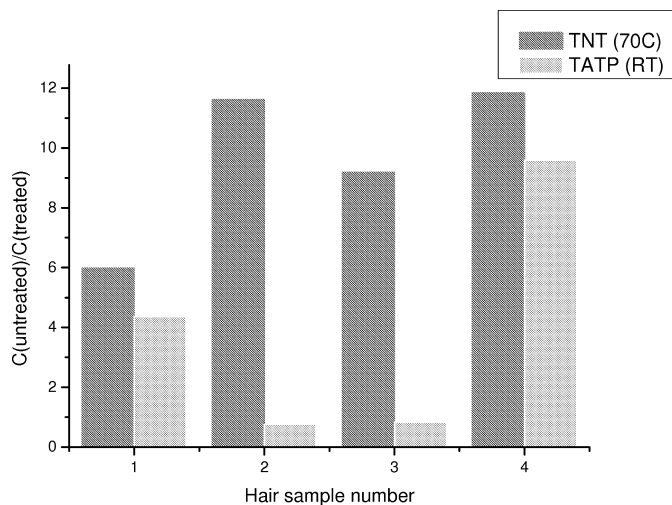


FIG. 5—Ratio of explosive sorption untreated to treated (methanol-KOH) hair.

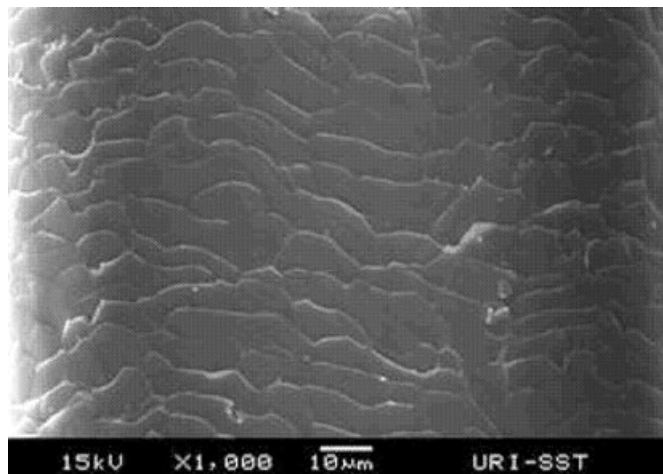


FIG. 8—Asian black hair treated with 8% H₂O₂ in 0.1 M NaOH.

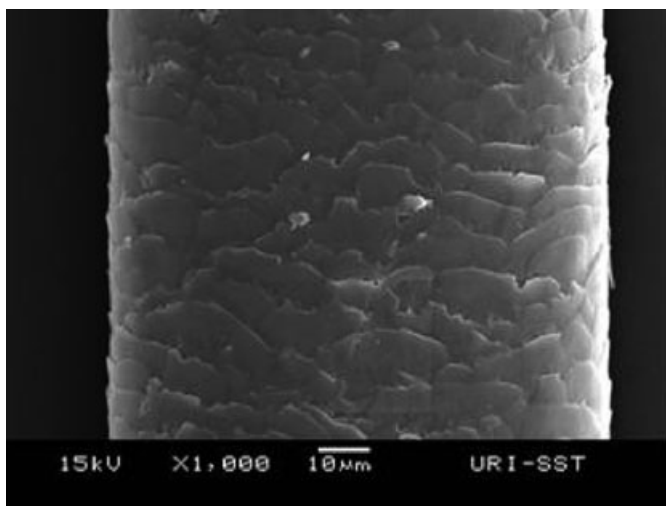


FIG. 6—Untreated Asian black hair.

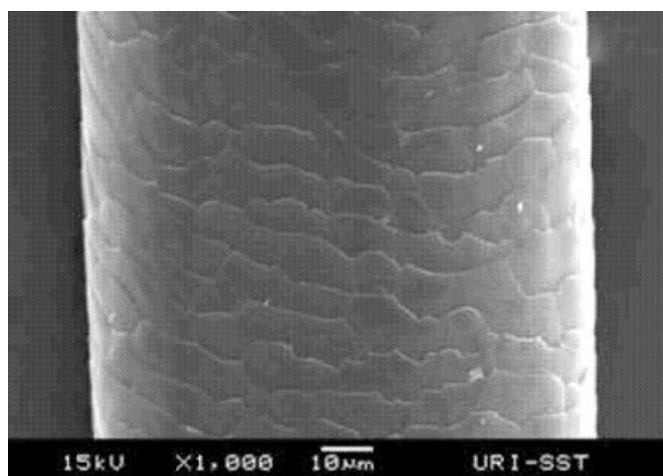


FIG. 9—Asian black hair treated with 0.1 M methanolic KOH.

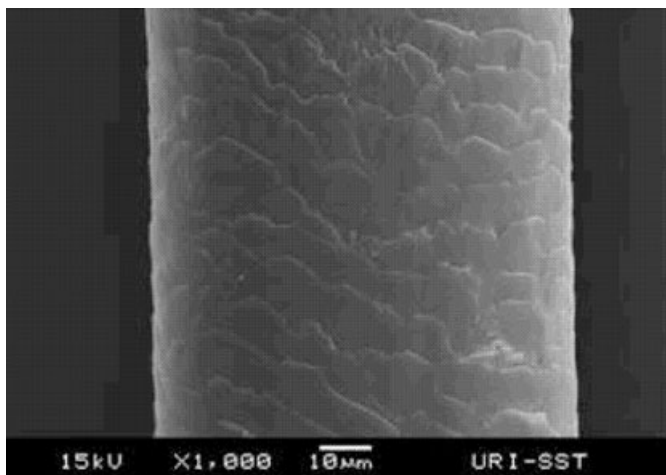


FIG. 7—Asian black hair treated with acetonitrile.

obtained for distilled water-rinsed samples, and the smallest variation for the sample treated by methanol-KOH solution. Note that at the scale edges, the largest phase changes are observed for all four samples. This might be due to enhanced sorption of water (or other solvent) along the scale edge.

A set of enlarged scans of these samples are presented in Fig. 11. The scans span $2 \times 2 \mu\text{m}$ and were performed on the surface of a single scale away from the scale edge. As observed in Fig. 11, the sample that was only treated with distilled water showed the largest surface roughness, while the one treated with methanol-KOH solution was by far the smoothest. These features are seen clearly in both height and amplitude images (left and middle columns). The phase change images show that, except in the case of the methanol-KOH treatment, where the hair surface was highly uniform, the samples exhibited small domains where elasticity is different from most of the surface. These results may indicate the complete removal of the 18-MEA layer in the case of the methanol-KOH treatment. However, the small domains with different elasticity may correspond not only to the presence of the 18-MEA layer but also to regions where solvent or humidity adsorbed efficiently.

Analysis of the height variation in these images (first column) is shown in Fig. 12. The analysis of height variation in the scanned

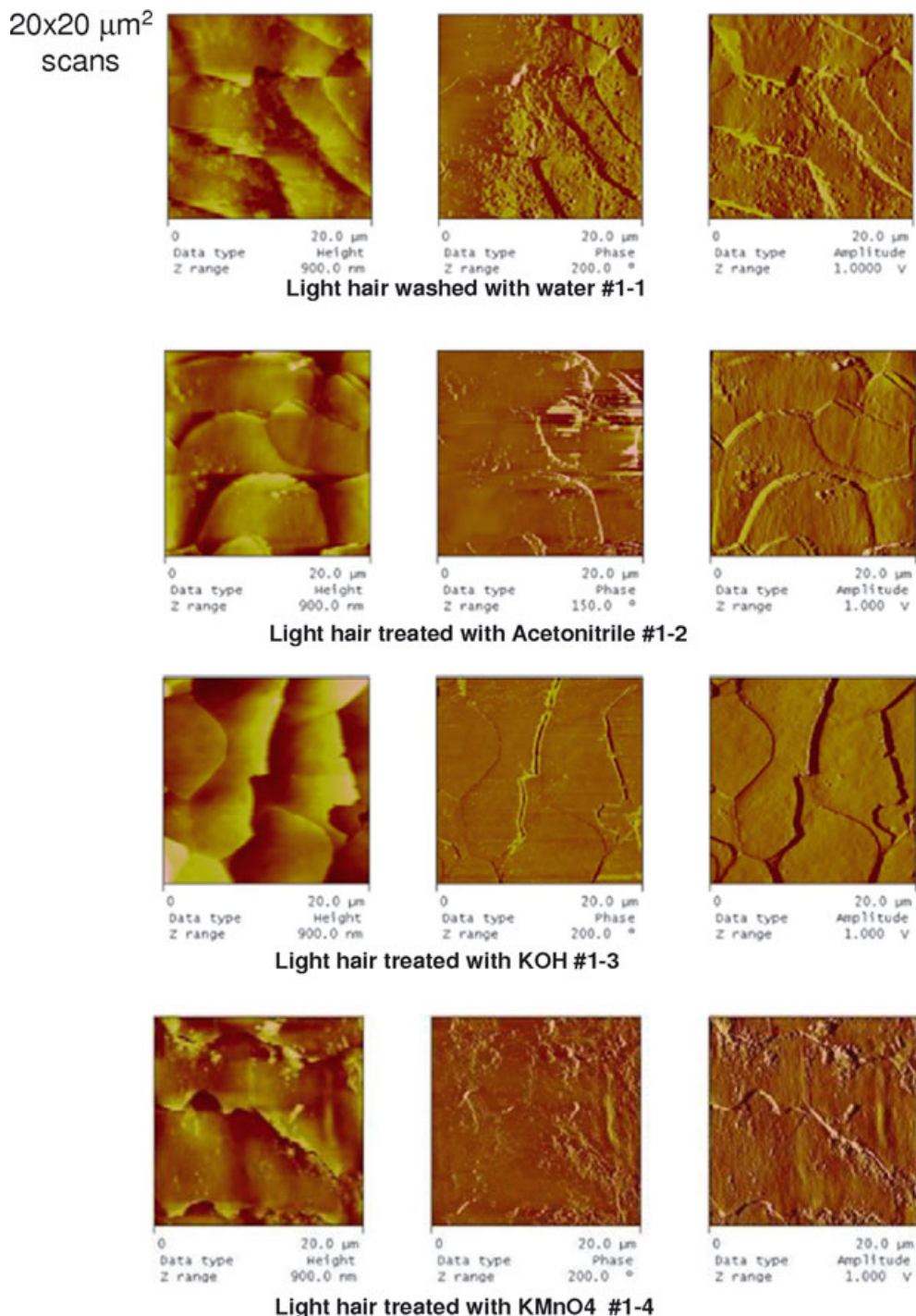


FIG. 10—Typical scans of hair samples treated in four solvents. The left column corresponds to height changes; the middle column, to amplitude changes; and the right column, to phase changes. The top row shows scans of hair treated in distilled water only; the second row was rinsed in acetonitrile; the third row was rinsed in methanol-KOH solution; and the bottom row was rinsed in permanganate solution.

region includes the mean value of the heights in the image, the root mean square height being defined by:

$$R_q = \sqrt{\frac{\sum_i Z_i^2}{N}}$$

and the arithmetic average of the absolute values of the surface height deviations measured from the mean plane, R_a , defined by:

$$R_a = \frac{1}{N} \sum_{i=1}^N |Z_i|$$

where N is the number of points whose height, Z_i , are measured in the scan.

Figure 12 shows the degree of roughness in these $(2 \mu\text{m})^2$ scanned areas. The principal measure is the value of R_a . In the case of samples rinsed in distilled water only, R_a equals 13.1 nm, while for methanol-KOH treatment, the observed value reduces to 1.8 nm.

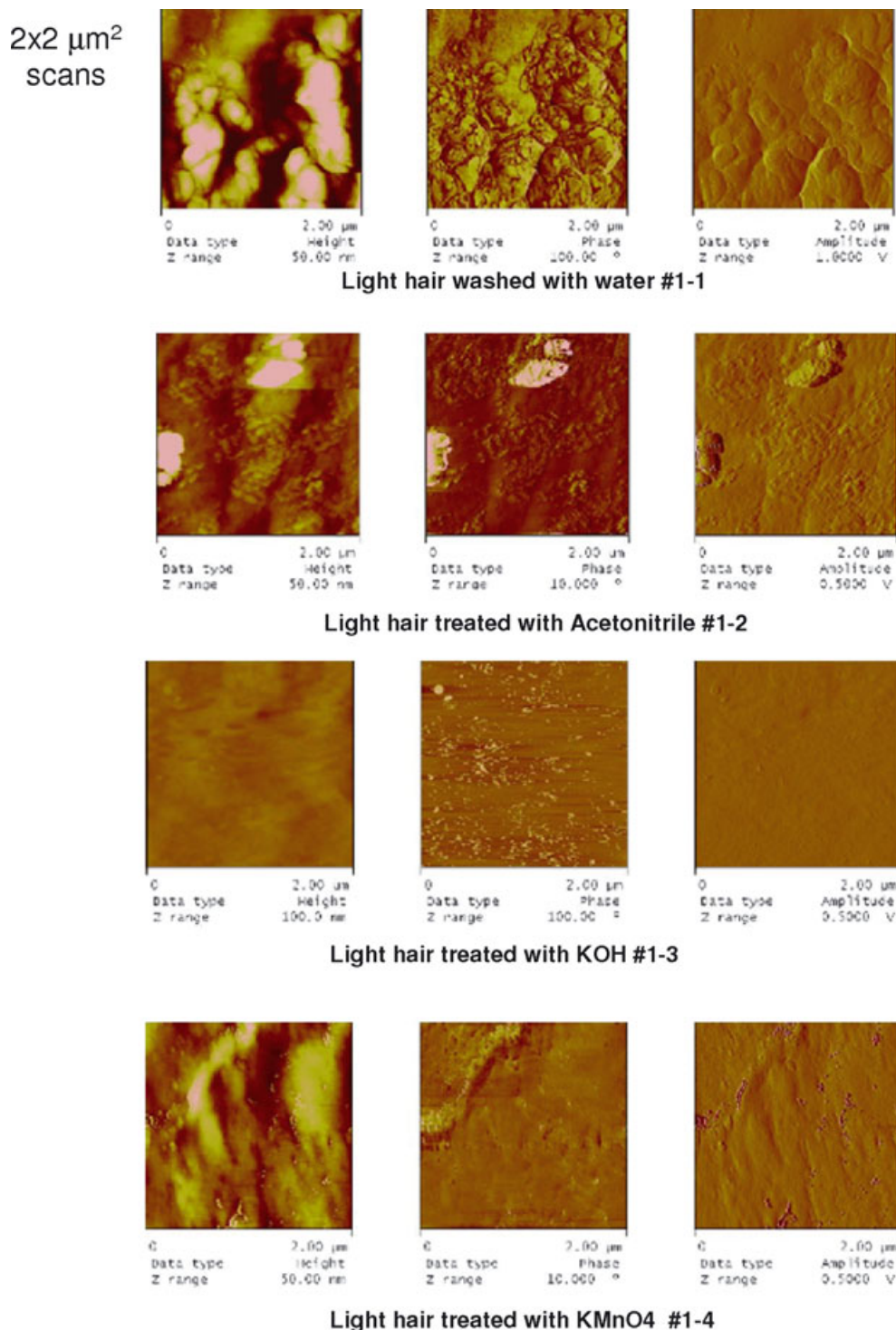


FIG. 11—Same format as Fig. 10, but the scan dimensions are 10 times smaller.

The corresponding values for the other two samples are in between these two values. The R_a value obtained for the methanol-KOH-treated samples seems to be even smaller than the width of the 18-MEA layer, another indication to its absence after the solvent treatment.

The TM-AFM photographs clearly show that all bleaching treatments examined reduce the hair surface roughness. This reduced roughness leads to a decreased sorption of both TATP and TNT on the hair surface. Yet, the sorption of these two explosives differs. Apparently, TATP nucleates more readily than TNT. DFT

calculations, described later, were used to determine possible mechanisms that may lead to TATP nucleation.

Possible Nucleation of TATP Microcrystals

Our previous study showed that TATP physisorption on acidic centers is thermodynamically stable (9): the hydrogen bonds formed in most complexes were quite long and led to very small changes in the geometry and electronic structure of the TATP

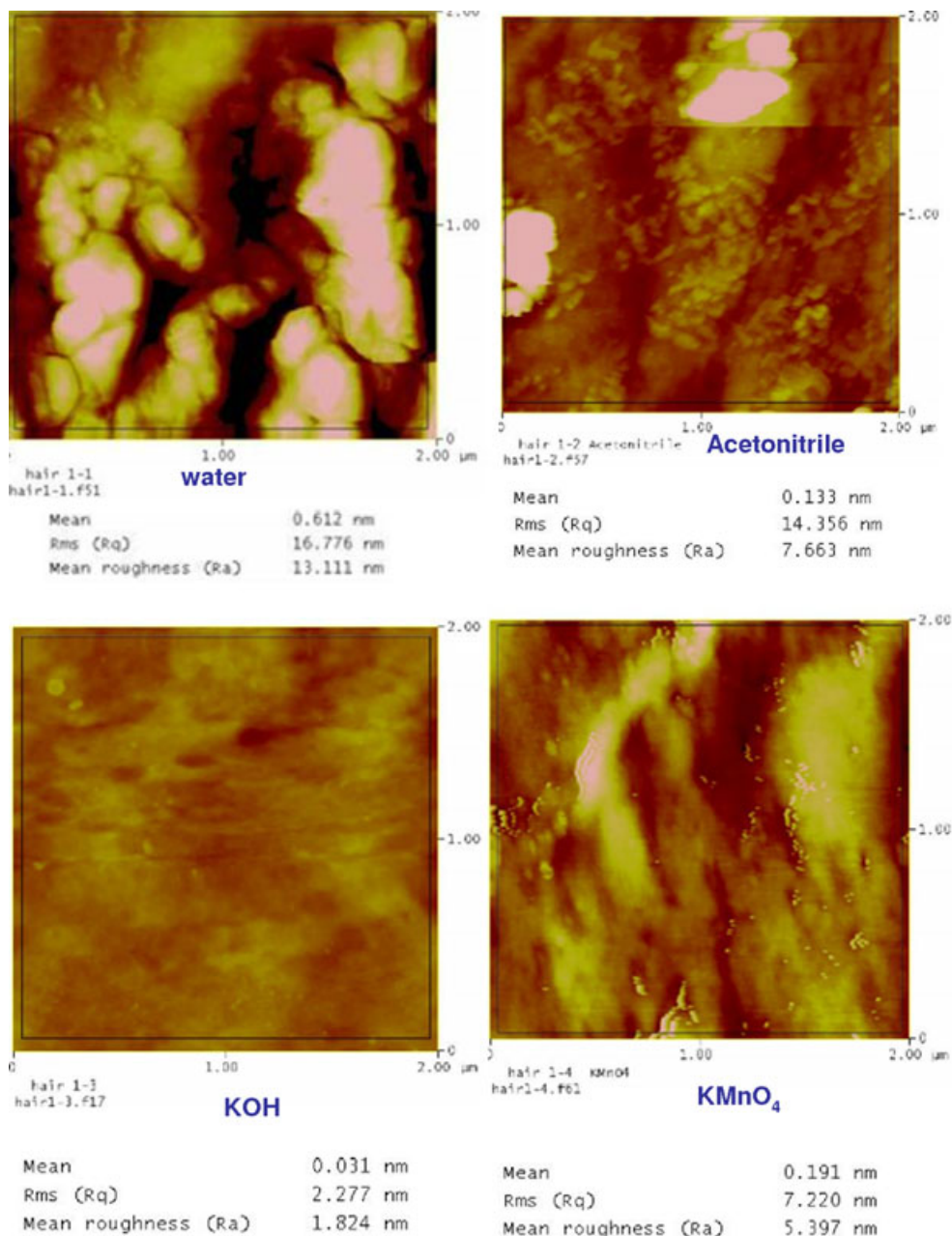


FIG. 12—Roughness measures of the four samples.

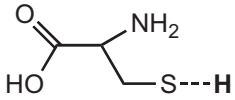
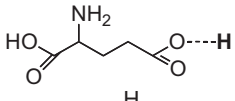
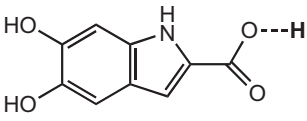
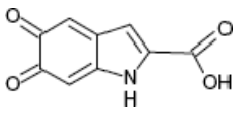
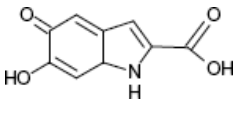
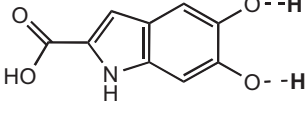
molecule. These results suggested that such sorption sites for TATP do not provide complexes that are stable enough to serve as nucleation sites. Furthermore, one would expect that nucleation sites will lead to much larger modification of the TATP structure and the charge distribution to provide efficient sorption of molecular TATP onto the modified adsorbed molecule. Hence, one must examine configurations in which the initial sorption leads to stable adsorbate that can induce further nucleation.

In the following, we compare the TATP sorption efficiency of different quinonic functional groups of melanin with those of glutamine and cystine units that are found on the hair protein surface (rows 1 and 2 in Table 4). These data clearly show that both phenolic and acidic OH groups of HQ form very strong hydrogen bonds with TATP. Such strong hydrogen bonding may lead to hydrogen transfer from the HQ to the adsorbed TATP.

Protonation of TATP is an exothermic process ($\text{TATP} + \text{H}^+ \rightarrow \text{TATP-H}^+$; $\Delta H = -216.0$ kcal/mol), leading to rupture of a C–O

bond to form a terminal O–H and a carbon radical (Fig. 13). The resulting three-coordinated C atom accepts large electron density (mainly from the nearest O atom) and forms nearly a double bond with it. The resulting complex exhibits bond elongation and reduction in interatomic population of the C–O bonds and strengthening of the O–O bonds. The HOMO of the complex is mainly localized on the O atoms marked with stars in Fig. 13 and has π^* nature with respect to this bond. However, proton abstraction by TATP from H_3O^+ is much less exothermic ($\text{TATP} + \text{H}_3\text{O}^+ \rightarrow \text{TATP-H}^+ + \text{H}_2\text{O}$; $\Delta H = -39.4$ kcal/mol). Proton abstraction from such weak acids as Cys and Glu is thermodynamically unfavorable ($\Delta H = +151.7$ and $+143.7$ kcal/mol; $\Delta G = +92.6$ and $+85.9$ kcal/mol, respectively). Such high endothermicity allows exclusion of TATP protonation by these sites on the hair surface. Chemisorption of the TATP molecule by addition of a S–H bond of Cys (Fig. 14) across the C–O bond was also found to be energetically highly unfavorable.

TABLE 4—DFT optimized hydrogen bond lengths (d_{O-H} , Å) and thermodynamic parameters (ΔH , kcal/mol and ΔG , kcal/mol at 298.15 K) for TATP interactions with functional groups of protein and melanin.

Group	Molecular Structure	Physisorption Properties		
		d_{O-H}	ΔH	ΔG^{298}
-SH	Cys 	2.370	-3.64	+7.19
-COOH	Glu 	2.327	-9.05	+5.16
-COOH	Hydroquinone (HQ) 	1.805	-19.10	-6.98
-COOH	Orthoquinone (OQ) 		-2.45	
-OH	Semiquinone (SQ) 	1.900	-4.99	
2(-OH)*	Hydroquinone (HQ) 	1.950; 2.145	-17.56	-4.54

TATP, triacetone triperoxide.

Another type of possible TATP activation is by interaction with radical centers present on the hair surface (cysteine) and in melanin granules. Radical interactions of TATP could proceed through several ways. Excitation of the molecule to the triplet state is thermodynamically unfavorable ($\Delta H = +33.02$ kcal/mol, $\Delta G^{298} = +25.95$ kcal/mol). Homolytic decomposition is highly endothermic ($\Delta H = +108.1$ kcal/mol), but abstraction of H atom by another radical can be energetically easier ($\Delta H = +0.8$ kcal/mol for hydrogen abstraction by an H atom). The preferential interaction of TATP with an H radical is attractive. It is characterized by a strong decrease in the product enthalpy (TATP + H [Fig. 15.I]: $\Delta H = -77.18$ kcal/mol, $\Delta G^{298} = -68.15$ kcal/mol; TATP + 2H [Fig. 15.II]: $\Delta H = -79.9$ kcal/mol, $\Delta G^{298} = -66.32$ kcal/mol). These interactions with a single or two H atoms lead to rupture of one O-O bond and elongation of the other O-O and several C-O bonds (Fig. 15). In the following, we shall term the products in these two reactions as product I and product II. The first interaction presents the formation of a radical nucleation center while the second one presents rupture of a radical chain. Exothermicities of these reactions are not enough to break the S-H bond in the cystine amino acid (reaction 1 in Table 5). Even the formation of a disulfide bond could not compensate the endothermicity associated with two H-atom transfer reactions (reaction 2 in Table 5). On the other hand, hydrogen abstraction reaction upon TATP sorptions onto SQ or HQ sites is energetically favorable.

The radical product I in reactions 3 and 4 (Table 5) exhibits higher affinity to form dimers with another TATP molecule (Fig. 16) than a closed shell TATP [ΔH for formation of (TATP)₂ and TATP-(I) dimers are -2.26 and -4.17 kcal/mol, respectively].

These results suggest that product I species may serve as possible nucleation sites for TATP if the gas phase is saturated with TATP. At room temperature, both TATP-TATP and TATP-(I) complexes become thermodynamically unfavorable as a result of the entropy effects. This is in agreement with the observed high vapor pressure of TATP at room temperature. Calculated ΔG^{298} values [$+8.42$ and $+8.08$ kcal/mol for (TATP)₂ and TATP-product I dimers, respectively] suggest that, in equilibrium with the saturated gas phase, TATP molecules will adsorb onto radical sites 1.77 times faster as compared to sorption onto the TATP crystallites that were clearly observed in our previous study (2). The dimer TATP-(I) remains a radical in nature; therefore, it continues to attract additional TATP molecules.

The most stable complex is formed between two product I radicals ($\Delta H = -29.40$ kcal/mol, $\Delta G^{298} = -10.64$ kcal/mol). This complex can also serve as a nucleation site for TATP; however, it does not possess a radical nature; hence, its ability to further adsorb additional TATP molecules should be similar to that of TATP crystallites.

The computational results discussed above allow exclusion of acidic and cystine/cysteine centers as possible TATP nucleation centers. From a chemical viewpoint, melanin centers are able to initiate nucleation of TATP microcrystallites. However, the fact that melanin granules are located inside the hair shaft makes such interaction unfeasible. Recently it was found that, despite the similar biochemical composition of human hair among different races (19,21), physico-morphological characteristics are not identical in different ethnic groups (27-29). In particular, (i) large melanin granules were found in black hair in the cortex layer (30,31) and (ii) the amounts of fibrous proteins and matrix substances differ in

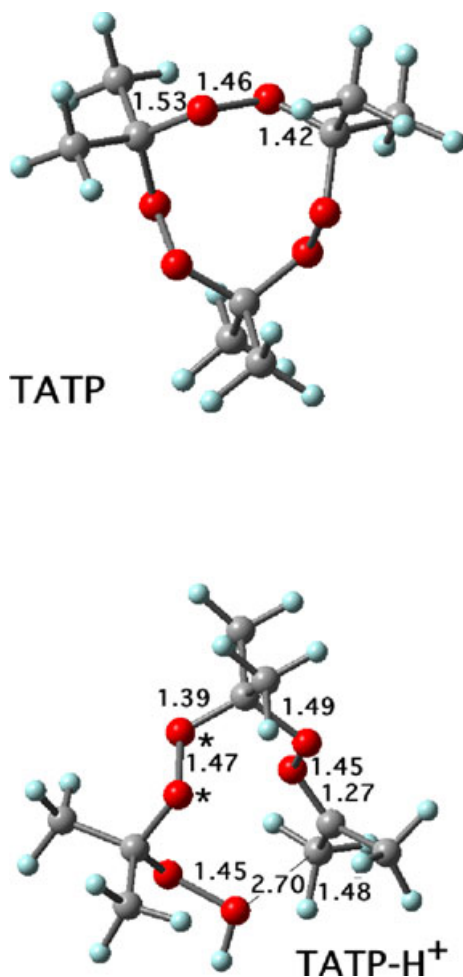


FIG. 13—Triacetone triperoxide (TATP) and TATP-H⁺ geometries optimized at the B3LYP/cc-pVDZ level of theory. Also shown are some important bond lengths.

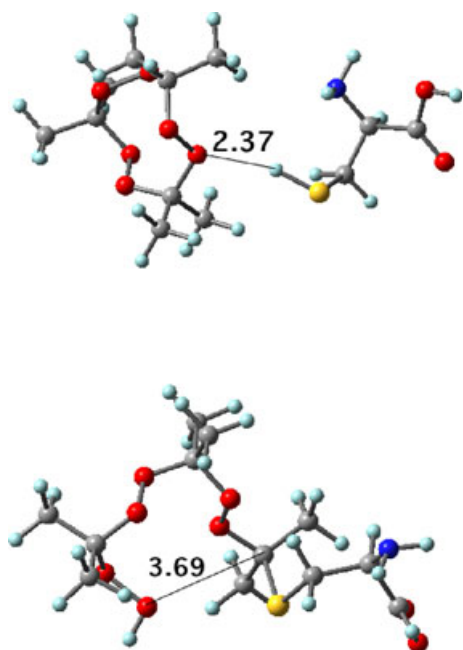


FIG. 14—Triacetone triperoxide interactions with cysteine (Cys): H-bond formation (top) and S-H addition across C–O bond (bottom).

the hair of different races (their ratios obtained from the Mongoloid hair were 0.45 ± 0.03 ; those from the Negroid, 0.18 ± 0.02 ; and those from the Caucasoid, 0.29 ± 0.02). These differences do not affect the distribution of the cystine-rich proteins (32). One would expect that penetration of molecules through the hair surface is more difficult for Asian origin hair as it has more cuticle layers and wider cuticle cells than Caucasian hair. In addition, the cuticular inclination of Asian hair is steeper and its cuticular interval is narrower than in Caucasian hair (33). However, a recent study demonstrated that the cuticles of Asian hair are more easily peeled off than Caucasian hair cuticles during daily grooming (34–36). This finding together with high abundance of melanin granules in the near-surface hair layers allows to suggest that interaction between melanin and TATP molecules takes place at defects or damage sites on black hair. This hypothesis is supported by wide individual variation in the sorption properties of black hair, which indicates random intra-individual physicochemical and structural variations not controlled in the experiments (see Table 1). Physisorption of explosive molecules within the lipid layer on hair surface could also provide nucleation centers at which explosive molecules can condensate in equilibrium with saturated gas phase to form nucleation centers for microcrystals. However, these centers are less active than radical centers. Significant acidity of sorption sites on melanin granule surface may play an important role in the coordination of explosive molecules at such sites prior to their nucleation. On the other hand, sorption of polar solvent molecules, such as acetonitrile and methanol, showing both hydrophilic and hydrophobic affinity, could result in blocking of most melanin nucleation centers present on hair surface. This is expected to markedly reduce radical-induced nucleation of TATP microcrystallites, whereas TNT sorption, which is driven preferentially by van der Waals and ionic interactions, should be only slightly affected.

Conclusions

In this study, hair was treated in a number of ways: moistening; rinsing with acetonitrile or methanol; bleaching with H₂O₂ and alkaline H₂O₂; and treating with a methanolic KOH solution or potassium permanganate. Bleaching the hair greatly reduced sorption of TATP and TNT to hair. However, treatments that had no effect on hair color had differing effects on TATP and TNT. For example, rinsing with acetonitrile or methanol drastically lowered the sorption of TATP, while having little effect on TNT. These observations, along with those previously reported in differential extraction experiments, may suggest that TATP attachment to hair is mainly a surface phenomenon, while TNT may have also an inner core sorption. The theoretical calculations discussed above may suggest that the experimental findings could also be related to the efficient sorption of solvent molecules to melanin sites. TM-AFM micrographs reveal surface structural changes as a result of the various treatments of hair. Together with the other results presented herein, this supports the hypothesis that 18-MEA lipid layer plays a major role in explosive sorption. DFT calculations were employed to explain the extremely high TATP sorption by several samples of black hair. It has been demonstrated above that TATP interactions with radical centers on melanin surface could lead to formation of microcrystallites when the hair is exposed to TATP saturated gas phase. The marked reduction of TATP sorption by pretreatment with acetonitrile or methanol is attributed by the calculations to blocking of the radical centers on the melanin granule surface. Reduced sorption of TATP and TNT to bleached and gray hair is attributed to both disappearance of radical centers and destruction of the lipid layer on hair surface. While the conclusions

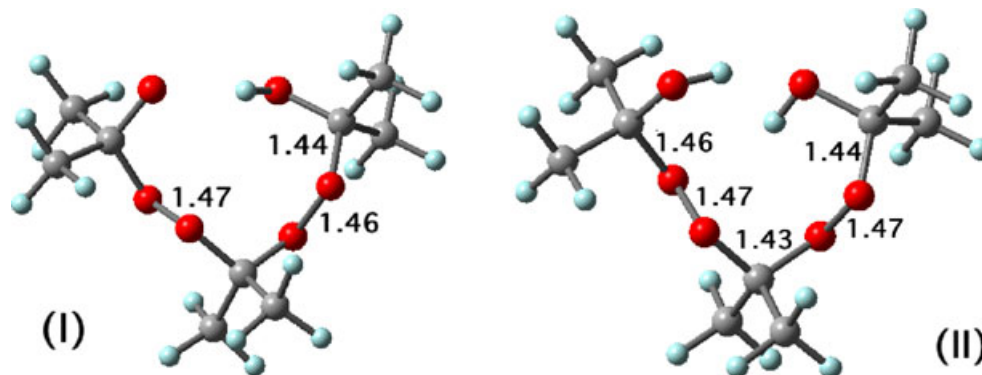


FIG. 15—Triacetone triperoxide (TATP)-H (I) and TATP-2H (II) geometries optimized at the B3LYP/cc-pVDZ level of theory. Also shown are some important bond lengths.

TABLE 5— Thermodynamics of H-atom abstraction by TATP.

		ΔH , kcal/mol	ΔG^{298} , kcal/mol
1	P-SH + TATP \rightarrow P-S+(I)	12.19	7.96
2	2Cys + TATP \rightarrow Cys2 + (II)	16.87	21.24
3	SQ + TATP \rightarrow OQ + (I)	4.99	-0.19
4	HQ + TATP \rightarrow SQ + (I)	-0.98	-6.38
5	HQ + TATP \rightarrow OQ + (II)	-28.89	-31.56
6	SQ + (I) \rightarrow OQ + (II)	-27.91	-25.18
7	HQ + (I) \rightarrow SQ + (II)	-33.88	-31.37

HQ, hydroquinone; OQ, orthoquinone; SQ, semiquinone; TATP, triacetone triperoxide.

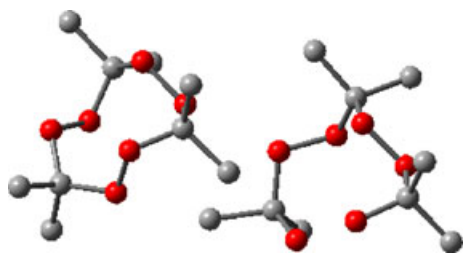


FIG. 16—Optimized (TATP-H-TATP) (complex TATP-I) dimer geometry. Hydrogen atoms are omitted for clarity. TATP, triacetone triperoxide.

described above are consistent with results of our experiments and theoretical calculations, they suggest additional experiments, which should lead to further substantiation.

References

- Oxley JC, Smith JL, Kirschenbaum L, Shinde K, Marimnganti S. Accumulation of explosives in hair. *J Forensic Sci* 2005;50(4):829–31.
- Oxley JC, Smith JL, Kirschenbaum L, Marimnganti S. Accumulation of explosive in hair: part 2. *J Forensic Sci* 2007;52(6):1291–6.
- Jones LN. Hair structure anatomy and comparative anatomy. *Clin Dermatol* 2001;19:95–103.
- Swift JA, Smith JR. Microscopic investigations on the epicuticle of mammalian keratin fibres. *J Microsc* 2001;204:203–11.
- Evans DJ, Leeder JD, Rippon JA, Rivett DE. Separation and analysis of the surface lipids of the wool fibre. In: Sakamoto M, Gakkai S, editors. Proceedings of the 7th International Wool Textile Research Conference; 1985 Aug 28–Sept 3; Tokyo, Japan: Society of Fiber Science and Technology Japan, 1985;135–42.
- Smith JR, Swift JA. Lamellar subcomponents of the cuticular cell membrane complex of mammalian keratin fibres show friction and hardness contrast by AFM. *J Microsc* 2002;206(3):182–93.

- Negri AP, Cornell HJ, Rivett DE. Model for the surface of keratin fibers. *Text Res J* 1993;63:109–15.
- Negri A, Rankin DA, Nelson WG, Rivett DE. A transmission electron microscope study of covalently bound fatty acids in the cell membranes of wool fibers. *Text Res J* 1996;66:491–5.
- Efremenko I, Zach R, Zeiri Y. Adsorption of explosive molecules on human hair surfaces. *J Phys Chem C* 2007;111:11903–11.
- Meredith P, Powell PJ, Riesz J, Nighswander-Rempel SP, Pederson MR, Moore EG. Towards structure-property-function relationships for eumelanin. *Soft Matter* 2006;2:37–44.
- Swift JA, Smith JR. Atomic force microscopy of human hair. *Scanning* 2000;22:310–8.
- LaTorre C, Bhushan B. Nanotribological characterization of human hair and skin using atomic force microscopy. *Ultramicroscopy* 2005;105:155–75.
- LaTorre C, Bhushan B. Nanotribological effects of hair care products and environment on human hair using atomic force microscopy. *J Vac Sci Technol* 2005;23:1034–45.
- Chen N, Bhushan B. Morphological, nanomechanical and cellular structural characterization of human hair and conditioner distribution using torsional resonance mode with an atomic force microscope. *J Microsc* 2005;220:96–112.
- Lodge RA, Bhushan B. Surface characterization of human hair using tapping mode atomic force microscopy and measurement of conditioner thickness distribution. *J Vac Sci Technol* 2006;24:1258–69.
- Frisch MJ, Trucks GW, Schlegel HB, Scuseria GE, Robb MA, Cheeseman JR, et al. Gaussian 03 revision C01wis5 (WIS customized version 5). Wallingford, CT: Gaussian Inc., 2004.
- Prota G. Melanins, melanogenesis and melanocytes: looking at their functional significance from the chemist's viewpoint. *Pigment Cell Res* 2000;13(4):283–94.
- Riley PA. Melanin. *Int J Biochem Cell Biol* 1997;29:1235–9.
- Kalyanaraman B, Felix CC, Sealy RC. Photoionization and photohomolysis of melanins: an electron spin resonance-spin trapping study. *J Am Chem Soc* 1984;106(24):7327–30.
- Wolfram LJ, Hall K, Hui I. The mechanism of hair bleaching. *J Soc Cosmet Chem* 1970;21:875–900.
- Kim BJ, Na JI, Park WS, Eun HC, Kwon OS. Hair cuticle differences between Asian and Caucasian females. *Int J Dermatol* 2006;45:1435–7.
- Robbins CR. Chemical and physical behavior of human hair, 3rd edn. New York, NY: Springer-Verlag, 1994;64–5,133–46.
- Hall K, Wolfram LJ. Isolation and identification of the hair protein component. *J Soc Cosmet Chem* 1975;26:247–54.
- Robbins CR, Kelly CH. Amino acid analysis of cosmetically-altered hair. *J Soc Cosmet Chem* 1969;20:555–64.
- Zahn H. Chemical processes in the bleaching of wool and human hair with hydrogen peroxide and peroxy acids. *J Soc Cosmet Chem* 1966;17:687–701.
- Breakspear S, Smith JR, Luengo G. Effect of covalently linked fatty acid 18-MEA on the nanotribology of the hair's outer surface. *J Struct Biol* 2005;149(3):235–42.
- Franbourg A, Hallegot P, Baltenneck F, Toutain C, Leroy F. Current research on ethnic hair. *J Am Acad Dermatol* 2003;48:S115–9.
- Menkart J, Wolfram LJ, Mao I. Caucasian hair Negro hair and wool: similarities and differences. *J Soc Cosmet Chem* 1984;35:21–43.

29. Lindelof B, Forslind B, Hedblad MA, Kaveus U. Human hair form. Morphology revealed by light and scanning electron microscopy and computer aided three-dimensional reconstruction. *Arch Dermatol* 1988;124(9):1359–63.
30. Taylor SC. Skin of color: biology structure function and implications for dermatologic disease. *J Am Acad Dermatol* 2002;46(2 Suppl. 2):S41–62.
31. Chakraborty DP, Shyamali R. Chemical and biological aspects of melanin. *Alkaloids Chem Biol* 2003;60:345–91.
32. Khumalo NP, Dawber RPR, Ferguson DJP. Apparent fragility of African hair is unrelated to the cystine-rich protein distribution: a cytochemical electron microscopic study. *Exp Dermatol* 2005;14(4):311–4.
33. Aubry AF. Applications of affinity chromatography to the study of drug-melanin binding interactions. *J Chromatogr B Analyt Technol Biomed Life Sci* 2002;768(1):67–74.
34. Joseph RE, Tsai WJ, Tsao LI, Su TP, Cone EJ. In vitro characterization of cocaine binding sites in human hair. *J Pharmacol Exp Ther* 1997;282:1228–41.
35. Slawson MH, Wilkens DG, Rollins DE. The incorporation of drugs into hair. *J Anal Toxicol* 1998;6:406–13.
36. Mars U, Larsson BS. Pheomelanin as a binding site for drugs and chemicals. *Pigment Cell Res* 1999;12(4):266–74.

Additional information and reprint requests:

Jimmie C. Oxley, Ph.D.
Chemistry Department
University of Rhode Island
Kingston, RI 02881
E-mail: joxley@chm.uri.edu